Applied Catalysis B: Environmental 99 (2010) 214–221

Contents lists available at ScienceDirect

Applied Catalysis B: Environmental

journal homepage: www.elsevier.com/locate/apcatb

Visible-light sensitive cobalt-doped $BiVO_4$ (Co-$BiVO_4$) photocatalytic composites for the degradation of methylene blue dye in dilute aqueous solutions

Bin Zhou[a,b,c], Xu Zhao[a], Huijuan Liu[a], Jiuhui Qu[a,*], C.P. Huang[c]

[a] Research Center of Eco-Environmental Sciences, Chinese Academy of Science, Beijing 100085, China
[b] Graduate School, Chinese Academy of Science, Beijing 100039, China
[c] Department of Civil and Environmental Engineering, University of Delaware, 352 Du Pont Hall, Newark, DE 19716, USA

ARTICLE INFO

Article history:
Received 9 March 2010
Received in revised form 7 June 2010
Accepted 10 June 2010
Available online 17 June 2010

Keywords:
Co-$BiVO_4$
Photocatalytic composite
Photodegradation
Methylene blue

ABSTRACT

A series of visible-light sensitive Co-$BiVO_4$ photocatalysts were synthesized by heteronuclear complexing method using diethylenetriamine pentaacetic acid (DTPA) as the chelating agent. The photocatalysts were characterized by X-ray diffraction (XRD), X-ray photoelectron spectroscopy (XPS), field emission scanning electron microscope (FESEM), UV–vis diffuse reflectance spectroscopy (DRS), and Raman spectroscopy. Results indicated that all Co-$BiVO_4$ photocatalysts had a crystal structure of monoclinic scheelite. Loading $BiVO_4$ with cobalt did not alter the crystal structure of the composites. Cobalt was present as oxides and was deposited on the surface of larger $BiVO_4$ particles. The oxidation state of cobalt varied with its content in Co-$BiVO_4$. The photocatalytic activity of Co-$BiVO_4$ was studied by the decolorization of methylene blue (MB). $BiVO_4$ containing 5% (molar wt) of cobalt exhibited the greatest photocatalytic activity with a 85% of MB removal versus 65% by pure $BiVO_4$ in 5 h. Factors such as pH, initial MB concentration, electrolytes, and irradiation conditions that may affect the photodegradation of methylene blue were studied. High pH and low initial MB concentration resulted in fast photocatalytic reaction. Electrolytes, especially those capable of scavenging hydroxyls, can inhibit MB degradation. The stability of the photocatalysts was confirmed using reclaimed Co-$BiVO_4$ in three successive runs. There was no loss of photocatalytic ability in three successive runs each of which lasted for 6 h with BM removal remained high at >90%. Results demonstrated clearly that Co-$BiVO_4$ was stable and resistant to photocorrosion during the photocatalytic oxidation of organic compounds such as methylene blue.

1. Introduction

Since the first study on the photocatalytic oxidation of organic compounds in aqueous system by Carey in 1976 [1], there have intensive investigations on the application of heterogeneous catalysis for the treatment of hazardous wastes [2,3]. Photocatalysis is based on the reactive properties of photogenerated electron–hole pairs. When a semiconducting catalyst is irradiated by a light with an appropriate wavelength, the electron–hole pairs are generated. The photogenerated hole, an electron donor, can react with the adsorbed water and OH^- group to form hydroxyl radical ($OH^\bullet$), whereas the photogenerated electron can react with oxygen to form superoxide radical ion ($O_2^{\bullet-}$). Both $OH^\bullet$, $O_2^{\bullet-}$ and the photogenerated hole are capable of oxidizing a host of organic and inorganic compounds [4]. TiO_2 is among the most studied semiconducting photocatalysts for the treatment of hazardous chemicals due to its superior photocatalytic ability, photo-stability, non-toxicity, low cost, and sparingly low water solubility [5,6]. Nevertheless, the high energy band gap of pure TiO_2 (e.g., 3.2 eV) limits its application because the electron–hole pairs can only be formed by UV light at wavelength shorter than 387 nm [7]. Thus, only a small portion of the solar spectrum can be utilized for photo-oxidation reaction using TiO_2. Additionally, the electrons and holes will undergo recombination rapidly, estimated at a rate of $(3.2 \pm 1.4) \times 10^{-11}$ cm^3 s^{-1}, if they are not consumed upon generation. The high electron/hole pair recombination rate reduces the quantum yield which is another major drawback in heterogeneous photocatalysis using TiO_2. Other semiconductors such as WO_3, SnO_2, ZnO, and CdS have large band gap as well and thus have limited application as TiO_2 [8].

In order to improve the solar conversion efficiency, there are many attempts to study visible-light sensitive catalysts. It has been reported that composite oxides containing the element of bismuth usually have strong response to visible light due to change of electronic structure in the photocatalytic composites. In a single-phase composite oxide, the Bi(6s) orbital is normally hybrid with the O(2p) orbital to form an up-shift valence band which results in band gap reduction [9]. There are numeral studies on the photocatalytic

* Corresponding author. Tel.: +1 302 831 8428.
E-mail address: huang@ce.udel.edu (J. Qu).

0926-3373/$ – see front matter © 2010 Elsevier B.V. All rights reserved.
doi:10.1016/j.apcatb.2010.06.022

property of Bi^{3+}-containing composites including bismuth titanate [10,11], bismuth germanate [12], bismuth tungstate [13,14], and bismuth molybdate [15,16]. Bismuth vanadate ($BiVO_4$) is a photoactive material used widely as an inorganic yellow pigment during the past two decades [17]. $BiVO_4$ can exist in three crystalline phases, namely, tetragonal zircon, monoclinic scheelite, and tetragonal scheelite. These three crystal types can undergo phase transition under different thermal conditions [18]. It has been reported that $BiVO_4$ in the form of monoclinic scheelite shows excellent photocatalytic performance under visible light [18]. In contrast with tetragonal BiO_4, which band gap is 2.9 eV, the monoclinic scheelite has a band gap energy of 2.4 eV and can absorb the solar spectrum up to the blue light fraction of ca. 520 nm [19]. Experimental results on the photocatalytic evolution of oxygen [20] and the photocatalytic degradation of organic compounds [21,22] using monoclinic BVO_4 indicated that BVO_4 was an effective photocatalyst under visible light. Nonetheless, although BVO_4 can utilize a greater portion of the solar light than TiO_2, the photogenerated holes and electrons recombine rapidly as well.

In order to deal with the above problems, there have attempts to doped $BiVO_4$ with transition and/or noble metallic ions as to enhance its photocatalytic sensitivity. Ge synthesized Pt/$BiVO_4$ [23] and Pd/$BiVO_4$ [24] by hydrothermal method and reported that the products exhibited significant increase in photocatalytic efficiency during the degradation of methyl orange. Kohtani et al. prepared a series of Ag-loaded $BiVO_4$ particles by an impregnation method and reported that Ag–$BiVO_4$ particles could decompose organic compounds such as 4-n-alkylphenol effectively under visible light in aqueous solutions [25].

Cobalt oxides such as CoO and Co_3O_4 are p-type semiconductors with unique electronic configuration and magnetic property. When cobalt oxides are in contact with an n-type semiconductor such as $BiVO_4$, a p–n junction is formed and the recombination of hole–electron pairs is suppressed. Long et al. [26] and Xu et al. [27] studied the photocatalytic properties of Co-doped $BiVO_4$ and reported a significant increase in the photoreactivity of $BiVO_4$. In this study, we prepared Co-doped $BiVO_4$ using the amorphous heteronuclear complexation technique. The heteronuclear complex precursor is stable and its chemical composition is easy to control comparing with that prepared by other methods such as solid-state reaction [28], sol–gel [29], coprecipitation [30], metalorganic decomposition [31], and solution combustion [32]. Furthermore, the crystallization step can be readily controlled at low calcination temperatures. Co-$BiVO_4$ particles with various cobalt contents and pure $BiVO_4$ were synthesized. The photocatalytic property of the catalysts was examined by studying the degradation of MB under visible light irradiation. Experimental parameters such as cobalt content, initial MB concentration, pH, degree of irradiation, and simple electrolytes that may affect the photodegradation efficiency were investigated as to establish the optimal condition for the photocatalytic system. Finally, the photocatalytic stability of the photocomposites was studied in multiple cycles using reclaimed catalysts.

2. Experimental

2.1. Preparation of catalysts

Co-$BiVO_4$ particles were prepared by amorphous heteronuclear complex according to the following procedures. The commercial Bi_2O_3 and V_2O_5 (analytical reagent grade) at a molar ratio of 1:1 were added to a beaker containing 80 mL of deionized distilled water while keeping the solution mixed with a magnetic stirrer. Diethylenetriamine pentaacetic acid (DTPA) was used as the ligand and added to the above solution at a molar ratio of DTPA:Bi:V = 1.5:0.5:0.5. The pH of the mixture was adjusted to about 11 using concentrated ammonia. $Co(NO_3)_2$, analytical reagent grade, was used as the hybrid metal ion. The concentration of Co in Co-$BiVO_4$ was 1%, 5%, and 10% (molar wt). The suspension was continuously stirred at 80 °C until all chemicals were dissolved completely and became a transparent and homogeneous solution. Then the solution was transferred to an oven and dried at 80 °C for 48 h as to evaporate the water. The final product of gel was calcined in a muffle furnace in air at 600 °C at a rate of 3 °C min^{-1} for 4 h and then cooled to room temperature. $BiVO_4$ particles without dopant were synthesized also following the same above steps and used in control studies.

2.2. Characterization of catalysts

The crystalline structure of the Co-$BiVO_4$ particles was examined with X-ray diffraction (XRD) recorded on a Rigaku D-Max B diffraction system with Cu Kα radiation (λ = 1.5405 Å) and graphite crystal monochromator. Survey scan was performed at a rate of 0.3° min^{-1} from 2θ = 15–80°. The accelerating voltage and applied current were 30 kV and 30 mA, respectively. X-ray photoelectron spectroscopy (XPS) was used to identify the elemental composition and the chemical state of Co-$BiVO_4$. Spectra were recorded with a PHI 5600 spectrometer using a monochromatic Al Kα X-ray source (beam energy 1486.6 eV) and a hemispherical electron energy analyzer. A pass energy of 58.7 eV for regional spectra was used. The absorption spectra of the photocatalysts, or UV–visible diffuse reflectance spectra, were obtained in the range of 200–750 nm at room temperature using a UV–visible spectrophotometer (Hitachi UV-3100) equipped with an integrating sphere attachment. $BaSO_4$ was used as the reflectance standard. Surface morphology and texture were observed with a field emission electron scanning microscope, FEESC (JSM-6700F, JEOL). The visible-light Raman spectra were recorded with a visible-light Raman spectrophotometer assembled by the Dalian Institute of Chemical Physics, Chinese Academy of Sciences. The surface charge of Co-$BiVO_4$ particles in aqueous solution was measured by a Zeta potential analyzer (Zetasizer 2000, Malvern).

2.3. Photodegradation experiments

Methylene blue (MB) was used to study the photocatalytic efficiency of Co-$BiVO_4$ illuminated by visible light. In this study, a square quartz cell with 45 mm in length and 80 mm in height was used as the photocatalytic reactor. A 150-W Xe lamp positioned atop the reaction vessel was used as the visible-light source. An optical filter (Model JB420, Shanghai Seagull Colored Optical Glass Co. Ltd., China) was placed in front of the lamp to allow the passage of light with wavelength longer than 420 nm. Co-$BiVO_4$ at an amount of 0.1 g was suspended in 100 mL of aqueous solution containing 10 mg L^{-1} of MB. The suspension was stirred continuously in darkness for 30 min prior to turning on the light as to assure equilibrium adsorption of MB by the photocatalyst. At given time intervals, 3 mL of the suspension were sampled and centrifuged to remove the photocatalytic particles from the aqueous solution as to obtain the supernatant for the analysis of residual MB. The concentration of MB was detected by recording the absorbance at characteristic band of 664 nm and by scanning the wavelength in the range of 300–800 nm using a Hitachi U-3010 spectrophotometer.

3. Results and discussion

3.1. XRD analysis of Co-$BiVO_4$ photocatalysts

The crystal composition and phase structure of the pure and Co-doped $BiVO_4$ particles were studied by XRD. After annealing at

Table 1
High resolution XPS analysis of Co($2p^{3/2}$) and Co($2p^{1/2}$).

Sample	Co(2p)		Splitting (eV)	Phases
	$2p^{3/2}$ (eV)	$2p^{1/2}$ (eV)		
$BiVO_4$-Co(1%)	780.5	798.0	17.5	CoO
$BiVO_4$-Co(5%)	779.7	796.3	16.6	Co_3O_4
$BiVO_4$-Co(10%)	778.9	794.2	15.3	Co_2O_3

600 °C for 4 h, all products exhibited sharp peaks indicating high degree of crystallinity during calcination. The structure of both the pure and Co-doped $BiVO_4$ were confirmed single monoclinic scheelite according to the Joint Committee on Powder Diffraction Standards (JCPDs 14-0688) with major characteristic XRD peaks detected at (2θ) 18.7°, 28.6°, and 30.5°. Therefore it was expected that all photocatalysts synthesized would have high photocatalytic efficiency due to their distinct monoclinic phase structure as reported previously [18,19]. Furthermore, results indicated that cobalt doping did not affect the crystal structure of $BiVO_4$ except only a slight decrease in the height of its major XRD peak at 28.6°. Therefore it can be concluded that the hybrid metal ion might be dispersed in the crystal at an amount too small to be detected or that the cobalt oxides might be loaded merely on the surface of $BiVO_4$ particles rather than being anchored within the lattice structure of $BiVO_4$.

3.2. The XPS survey of M-$BiVO_4$ photocatalysts

XPS is a useful tool for identifying the chemical state of various hybrid species in the Co-$BiVO_4$ composite oxide. Fig. 1 shows the profile of high-resolution XPS survey of cobalt in the catalyst composite. Table 1 lists the main signals of Co($2p^{3/2}$) and Co($2p^{1/2}$) doublets. It is obvious that the binding energy of Co($2p^{3/2}$) and Co($2p^{1/2}$) were decreased when the cobalt content in the Co-$BiVO_4$ composite was increased. The splitting between these two orbitals also decreased from 17.5 to 15.6 eV. Comparing the binding energy of Co($2p^{3/2}$) was reported by Wagner et al. [33] it was found that cobalt was present as oxide in Co-$BiVO_4$ composites and the oxidation state varied with the cobalt content. Cobalt was present as CoO, Co_3O_4, and Co_2O_3 when the cobalt content was 1%, 5%, and 10%, respectively. Note that Co_3O_4 is the hybrid cobalt oxide of CoO and Co_2O_3, i.e., a tetrahedral Co^{2+} and an octahedral Co^{3+} contributing to the Co(2p) spectral region [34]. Accordingly, the valence of cobalt in the composites changed gradually from +2 to +3 as the cobalt content was increased from 1% to 10%. The decrease in the Co($2p^{3/2}$) and Co($2p^{1/2}$) spin–orbit splitting was caused by the decrease of unpaired electrons. Besides the main signal of Co(2p), an adjacent shake-up structure at higher binding energy was also observed. The formation of the shoulder is often interpreted as result of metal–ligand charge transfer.

3.3. SEM imaging of Co-$BiVO_4$ photocatalysts

The morphology and microstructure of the Co-$BiVO_4$ photocatalysts were observed with field-emission scanning electron microscopy (FESEM). Fig. 2 shows the FESEM images of the pure and Co-doped $BiVO_4$ photocatalysts. It can be seen that the shape of both the pure and cobalt-doped $BiVO_4$ particles were irregular. The size of the secondary particles varied from 0.3 to >1.0 μm. It must be mentioned that photocatalytic particles of large geometric dimension are more suitable for application to the treatment of hazardous chemicals in liquid wastes due to the simplicity and easiness in solid–liquid separation and thus with much improved workability for the photocatalysts. The surface of pure $BiVO_4$ was smooth. After cobalt doping, it is seen that there were smaller particles of various size dimensions scattered over the surface of the larger $BiVO_4$ particles. As the cobalt content was increased, both the number and size of the mixed particles increased. The small particles in the size range of <100 nm were presumably cobalt oxides that formed the hetero-junction structure of the composite $BiVO_4$ particles at the interface.

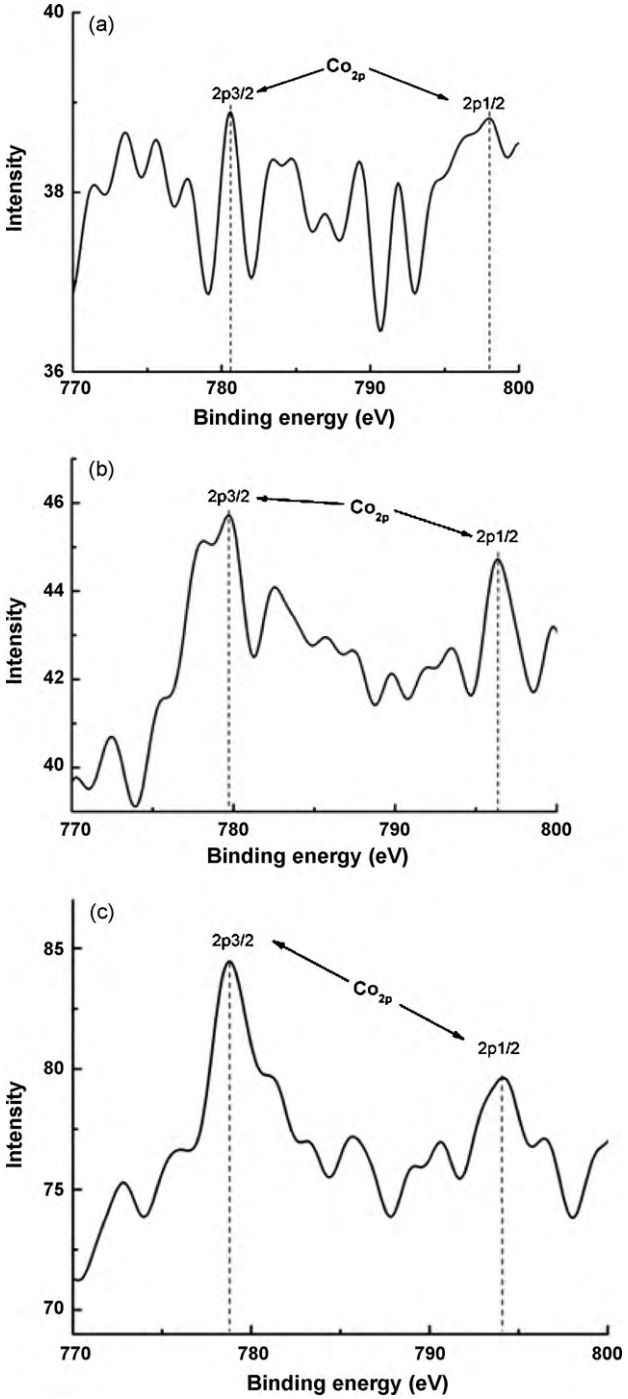

Fig. 1. High resolution of XPS patterns of Co(2p): (a) $BiVO_4$-Co(1%), (b) $BiVO_4$-Co(5%), and (c) $BiVO_4$-Co(10%).

The energy-dispersive X-ray spectroscopy (EDX) was used to study the surface element composition of Co-$BiVO_4$ photocatalysts. The result showed that the molar ratio of Co to Bi was 10.2%, 22.8%, and 27.8% at cobalt content of 1%, 5%, and 10% (molar wt), respectively. The Co to Bi ratio increased exponentially with cobalt content.

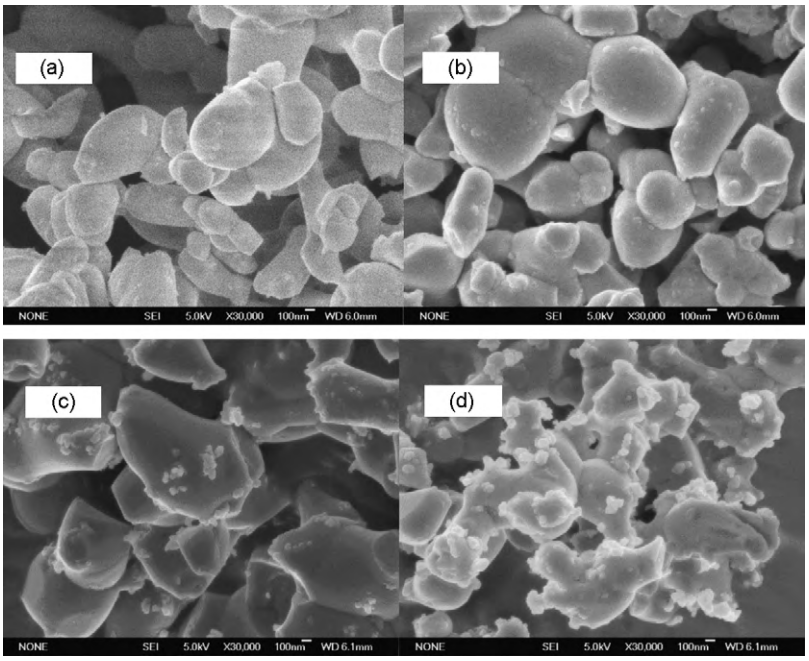

Fig. 2. FESEM images of (a) pure $BiVO_4$, (b) $BiVO_4$-Co(1%), (c) $BiVO_4$-Co(5%), and (d) $BiVO_4$-Co(10%).

3.4. UV–vis absorption spectra of Co-$BiVO_4$ photocatalysts

Fig. 3 shows the UV–vis diffuse reflectance spectra of the pure and Co-doped $BiVO_4$ catalysts. All samples exhibited strong absorbance. A characteristic pattern of metal oxides can be seen. All light absorbance profiles had a trailing edge in the near-UV range indicating direct band gap of the semiconductors. It is also noted that the light absorbance increased dramatically when the wavelength was decreased from the near-UV to the UV region. The sharpness of the spectrum is related to band gap transition. It is clear that doping $BiVO_4$ with cobalt tended to increase the light absorption in the UV and near-UV region. At a cobalt content of 10%, Co-$BiVO_4$ expressed the highest light absorption intensity. Increase in cobalt content resulted in a red-shift by the $BiVO_4$ photocatalytic composite. The absorption edge of pure $BiVO_4$ was at ca. 525 nm. The edge was extended from 525 to nearly 550 nm when the cobalt content was increased from 0 to 10%. It is well known that the optical absorption property of an oxide semiconductor is related to its electron configuration. This red-shift in light absorption could be attributed in part to a transition of charge-transfer between the cobalt ions and the conduction or the valance band of $BiVO_4$. The band gap energy (eV) can be obtained by the Kubelka-Munk function based on the diffuse reflection spectral data [35], i.e., $A\hbar\nu = c(\hbar - E_g)^n$, where A is the absorption coefficient, $\hbar\nu$ is the photon energy, c is a constant ($c = 1$), and E_g is the band gap energy. In the above equation, n is a constant and is dependent on the type of semiconductor. In the case of $BiVO_4$, n is equal to 0.5 and 2 for direct and indirect band gap, respectively [26]. The band gap for the pure and Co-doped $BiVO_4$ was estimated to be 2.44, 2.43, 2.42, and 2.39 eV at cobalt content of 0, 1%, 5%, and 10%, respectively. Doping cobalt has narrowed the band gap linearly. Scrutinizing the band gap in the visible light region where considerable light absorption occurs, one can expect significant photoreaction by the catalyst composites under sunlight irradiation.

3.5. Raman spectra

Raman spectroscopy is helpful to examining the local structure of the synthesized Co-$BiVO_4$ composite particles. The Raman spectrum was recorded from wave number in the range of 150–1200 cm^{-1}. Fig. 4 shows the Raman spectra of the catalyst composites. All four $BiVO_4$ composites exhibited Raman bands at 330, 365, and 826 cm^{-1} which are characteristic of the monoclinic scheelite structure [36]. The single band at around 826 cm^{-1} is normally attributed to the symmetric V–O stretching mode (A_g symmetry). There was a small Raman band shift towards the low end of the spectra near 826 cm^{-1} in all four samples which implies that the average short-range symmetry of the VO_4 tetrahedra was rendered more organized upon cobalt doping. A weak shoulder at about 718 cm^{-1}, next to the 826 cm^{-1} peak, can be assigned to the anti-symmetric V–O stretching mode [37]. The bands at ca. 365 and 333 cm^{-1} are attributed to the symmetric V–O (A_g) bending mode and the anti-symmetric V–O (B_g) bending mode of the VO_4 units, respectively [38]. The signal at 365 cm^{-1} is stronger than that at 333 cm^{-1}, because the symmetry defaults in the VO_4 tetrahedral are more than those of the anti-symmetry mode. The peak positioned at 205 cm^{-1} can be attributed to the external modes (rotation/translation). The intensity of the peaks decreased with increase in cobalt content. This can be attributed to the Raman spectroscopic technique which can only examine the surface structure of a sample. Furthermore, as the cobalt content was increased there was formation of heteroparticles at larger number and broader range in size distribution. These smaller heteroparticles tended to spread over the surface of the larger $BiVO_4$ particles, reduced the area of $BiVO_4$ for direct exposure to the Raman light spectrum, and resulted in a weakening of the light signal received by the photocomposite.

4. Photocatalytic degradation of MB

The photocatalytic capability of the Co-$BiVO_4$ composites was studied by the removal of methylene blue using the Co-$BiVO_4$ catalysts synthesized under various conditions including pH, initial MB concentration, supporting electrolytes, and irradiation status.

4.1. Effect of cobalt content

Fig. 5 shows results of the effect of cobalt content on the decoloration of MB as a function of irradiation time. The photo-

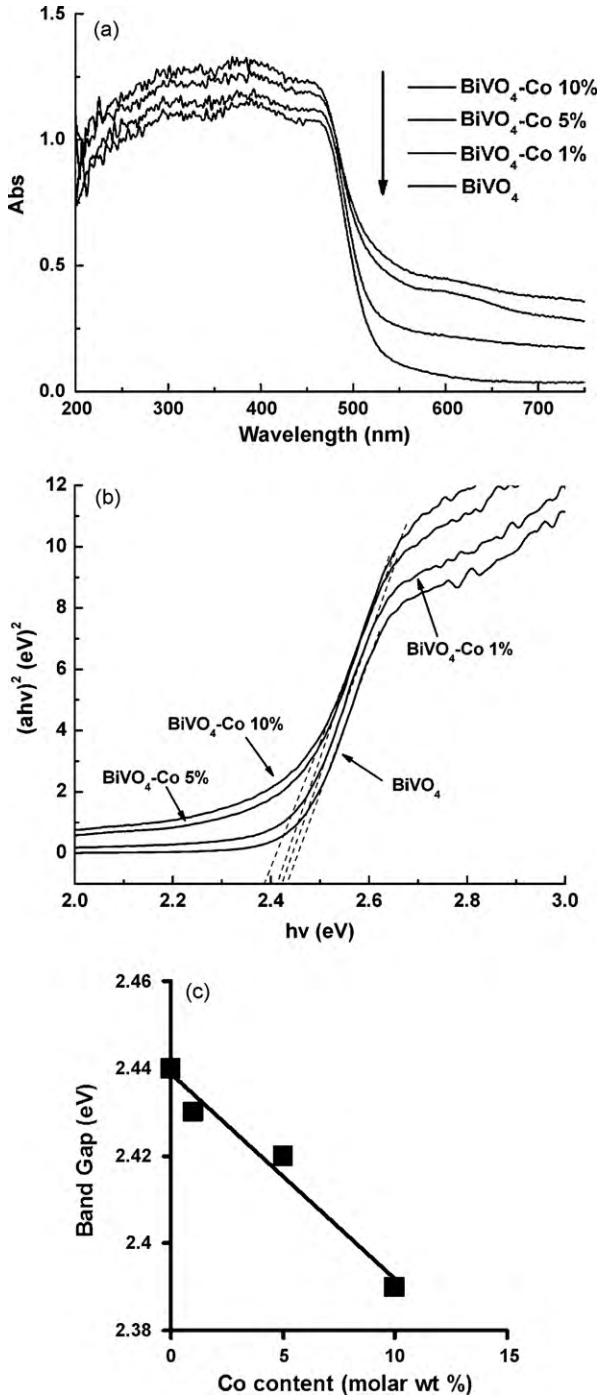

Fig. 3. UV–vis diffuse absorption spectra (a) and the estimated band gap (b) of the pure and the Co-$BiVO_4$ composite photocatalysts.

catalysts only removed 2% of MB in dark after a reaction time of 30 min. The percent photocatalytic decoloration of MB was 65%, 78%, 80% and 85% when the cobalt content was 0, 1%, 5%, and 10%, respectively, in 5 h under light irradiation. The result indicated that the cobalt content played an important role on the photocatalytic activity of $BiVO_4$. Cobalt oxides are p-type semiconductors whereas $BiVO_4$ is an n-type solid state. If the work functions of the cobalt dopants were higher than that of the $BiVO_4$, by loading the cobalt oxide on $BiVO_4$ a p–n heterojunction, i.e., a Schottky barrier, is formed at the interface where the former acts as an electron trap. When the Co-doped $BiVO_4$ is irradiated by a light with energy higher than the band gap, the electrons are excited from

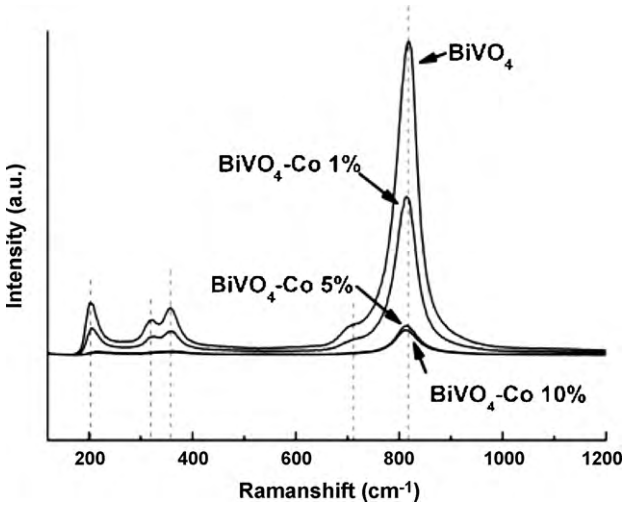

Fig. 4. Raman spectrum of the pure and the Co-$BiVO_4$ composite photocatalysts.

the valence band to the conduction band, transfer across the Co-$BiVO_4$ interface and arrive at the cobalt oxides, and then become trapped by the positively charged cobalt ions. The Schottky barrier makes it difficult for the photogenerated electrons to return to $BiVO_4$ and become recombined with the photogenerated holes. Ultimately, the trapped electrons are scavenged by the adsorbed oxygen molecules to produce superoxide radicals. The holes are left in the valence band of $BiVO_4$ after the departure of excited electrons and act as oxidants for the target pollutants.

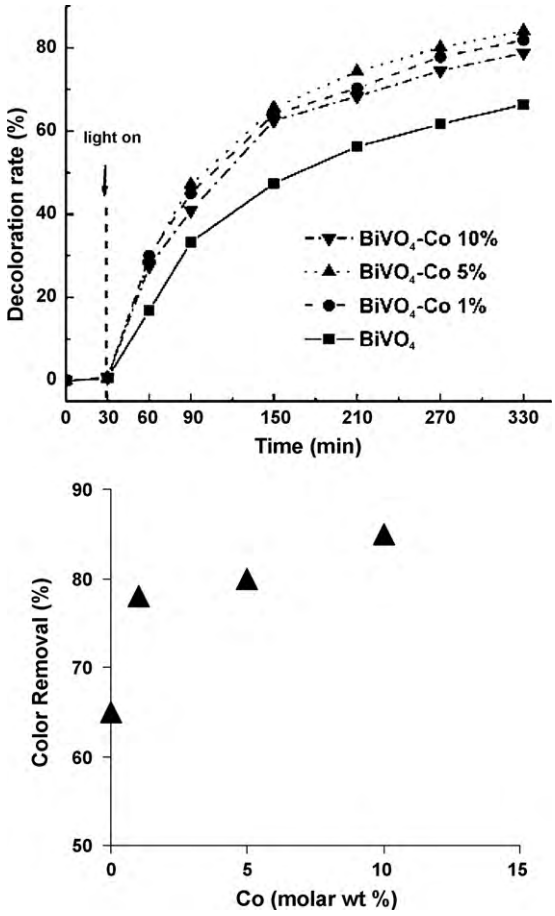

Fig. 5. Effect of cobalt content on the decolorization of MB at $\lambda > 420$ nm and pH 7.

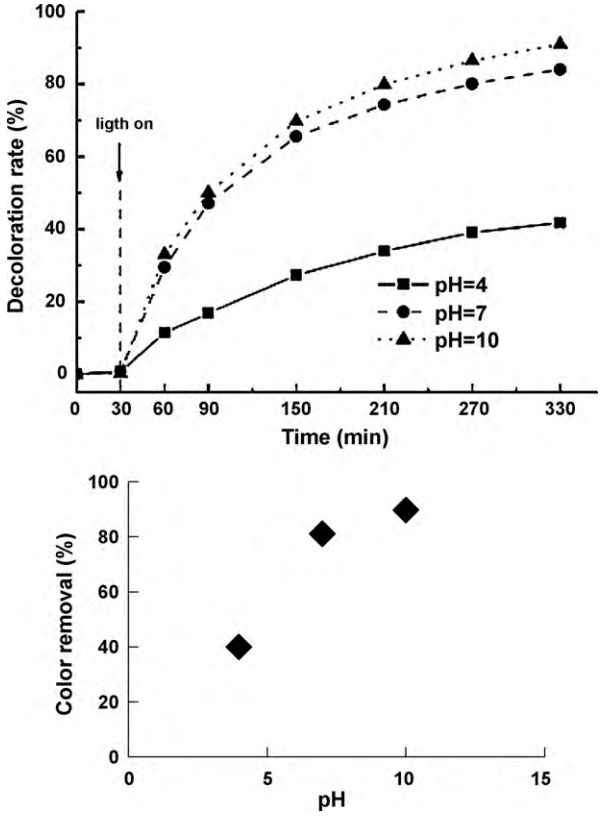

Fig. 6. Effect of pH on the decolorization of MB at λ > 420 nm.

Results show clearly that cobalt content is crucial to photoreactivity. The optimum cobalt content for the photocatalytic decoloration of MB appeared to ca. 5%. Further increase in cobalt content only resulted in slight increase in the photocatalytic decoloration of MB, however. Doping cobalt at the optimum amount can lead to the dispersion of fine cobalt oxide particles on the $BiVO_4$ surface evenly and enhance photoactivity. The cobalt oxides tended to agglomerate into large bulk aggregates at high cobalt content as seen from the FESEM images and resulted in slight increase in photocatalytic activity. Further covering the surface of the $BiVO_4$ photocatalyst by clusters of cobalt oxides also reduced the area directly exposing to the incoming light. The presence of excessive number of cobalt oxide particles can create hole–electron recombination centers and reduce the efficiency of charge separation. On the opposite, low cobalt content yields less charge trapping centers for the photogenerated electrons and the rate of hole–electron recombination will increase.

The oxidation state of cobalt can be another important factor affecting the photodegradation of dye. The XPS spectra indicate that the valence of cobalt changed from +2 to +3 as the cobalt content was increased. Co_3O_4 was the major cobalt oxide which has both +2 and +3 oxidation states at cobalt content of 5%. Presumably, the hybrid valence nature of cobalt might be better trapper for the photogenerated electrons than that of single oxidation state.

4.2. Effect of pH

Fig. 6 shows the effect of pH on the removal of MB by the Co-$BiVO_4$ photocatalysts. The pH_{zpc} of Co-$BiVO_4$ was 4.5 indicating that the catalyst will be positively charged when the pH is lower than 4.5 and negatively charged when the pH is greater than its pH_{zpc} (Fig. 9). Intuitively MB, a cationic dye [39], can be adsorbed easily on

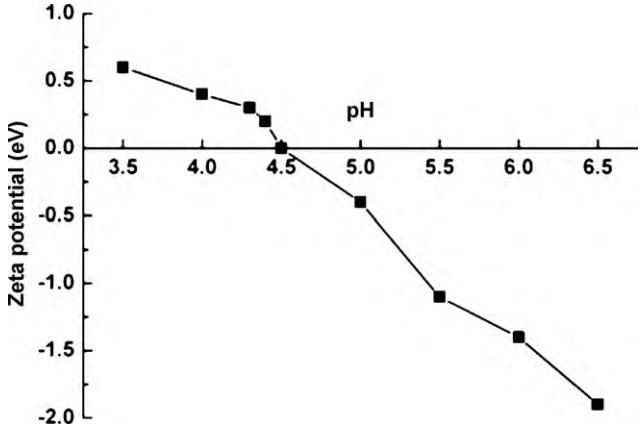

Fig. 7. Zeta potential of $BiVO_4$-Co(5%) as a function of solution pH.

the surface of the negatively charged catalyst at $pH > pH_{zpc}$. Adsorption of MB on the composite surface reduces the recombination rate of photogenerated charge carriers and accelerates the interfacial charge transfer process. Upon visible light irradiation for 5 h, the percent of MB decoloration was 40%, 81%, and 90% at pH of 4, 7, and 10, respectively. There was only slight increase in color removal when the pH was increased from 7 to 10. Although strong adsorption of the dye took place at high pH, excessive MB adsorption may block light from arriving at the catalyst surface, reduce the surface light intensity, and impede the hole-electron photoexcitation process subsequently. Furthermore, the concentration of hydroxyl radicals in solution is decreased at high pH which will decrease the rate of photoxidation. Both the catalyst surface and the dye are positively charged at pH 4, therefore the extent of MB adsorption is negligible due to strong electrostatic repulsion which will decrease the color degradation rate. First, the functional groups of MB, namely –C=S and –C=N, can undergo hemolytic cleavage readily [40]. Then attack of the intermediates by the hydroxyl radicals generated photocatalytically lead to MB removal finally. Moreover, less hydroxyl radicals are generated under acidic condition which will result in less MB decoloration (Fig. 7).

4.3. Effect of initial MB concentration

The effect of initial MB concentration on the degradation rate was investigated at three initial dye concentrations of 5, 10, and 25 mg L^{-1}. Fig. 8 shows color degradation as a function of irradiation time at three initial concentrations. In 5 h, the percent color degradation increased from 42 to 82 then to 97% when the initial MB concentration was increased from 5 to 10 then to 25 mg L^{-1}, respectively. The percent of color removal reached a maximum value of ca. 97% at an initial MB concentration of ca. 15 mg L^{-1} then remained unchanged when the initial MB concentration increased to >15 mg L^{-1}. Based on the present experimental conditions and results presented in Fig. 9, it is possible to estimate the quantum yield. At a 5-h reaction time, the quantum yield was ca. 0.01, 0.026, and 0.081 at initial BM concentration of 5, 10 and 25 mg L^{-1}, respectively. The results were in the same order of magnitude as those reported by Schiavello et al. [41] and Cornu et al. [42]. Schiavello et al. reported a quantum yield of 0.0186–0.0284 for the photolysis of water [41], whereas Cornu et al. reported a quantum yield of 0.01–0.05 for the photocatalytic oxidation of formate usingTiO_2 photocatalyst [42]. It is believed that increase in MB concentration affects light penetration through the solution. The degree of light penetration at high initial concentrations is reduced which will result the arrival of less photons at the catalyst surface. Intermediates formed during photocatalytic oxidation of the parent dye

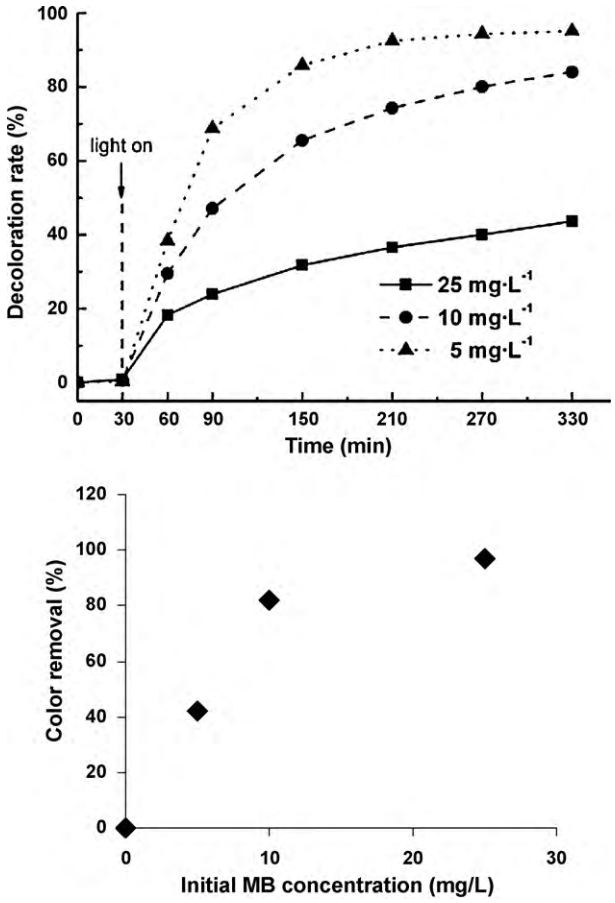

Fig. 8. Effect of initial MB concentration on the decolorization of MB by $BiVO_4$-Co(5%) photocatalyst at $\lambda > 420$ nm and pH 7.

can interfere with the degradation of the later. Dye molecules and intermediates tend to compete with each other for limited adsorption and catalytic sites on the Co-$BiVO_4$ surface which inhibits the decoloration of the former [43]. Competition between parent dye compounds and intermediates was enhanced at high MB concentration due to increase in the production of degradation intermediates.

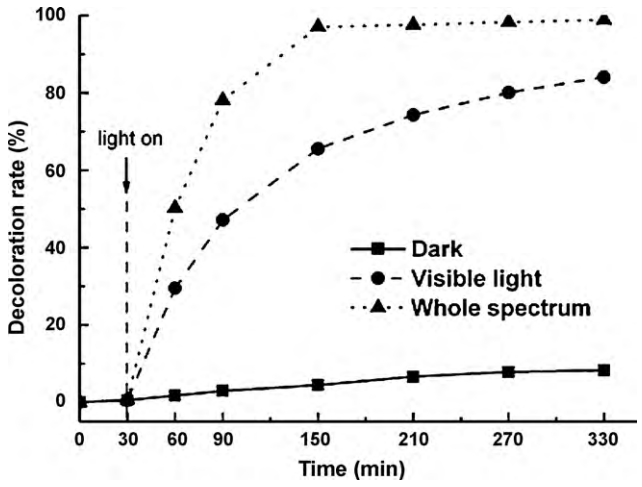

Fig. 9. Effect of visible light irradiation condition on the decolorization of MB by $BiVO_4$-Co(5%) photocatalyst at pH 7.

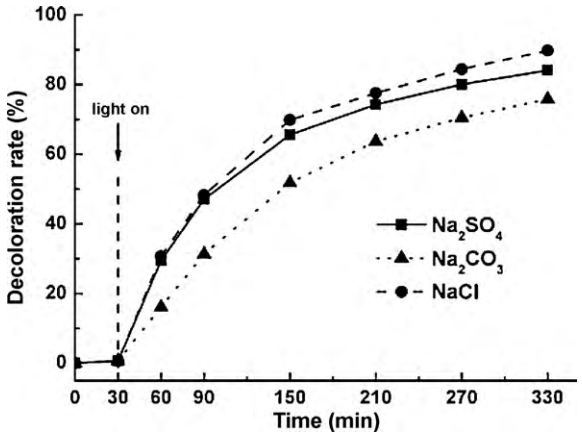

Fig. 10. Effect of electrolyte on the decolorization of MB by $BiVO_4$-Co(5%) photocatalyst at pH 7.

4.4. Effect of light irradiation condition

Sun is the cheapest and most abundant source of energy. Sunlight will be the best and final choice of energy source for large-scale implementation and operation heterophotocatalytic system. The decoloration of MB was studied with and without the optical filter being placed in front of the Xe lamp. Without the optical filter, the Co-$BiVO_4$ catalyst was exposed to the full spectrum of the Xe lamp. Fig. 9 shows the result of MB degradation under different illustration condition exemplified by the $BiVO_4$-Co(5%) photocatalyst. Nearly 100% of MB was removed from the solution in 2 h when the Co-$BiVO_4$ film was directly exposed to the Xe lamp, i.e., full spectrum, whereas only 85% of the dye was degraded after 5 h when the Co-$BiVO_4$ particles were illuminated by visible light ($\lambda > 420$ nm). Note that the percent of dye degradation under dark condition was less than 10%. In the heterophotocatalysis system, only the photons with energy higher than that of the band gap can be absorbed by the catalyst and utilized to generate holes. The shorter the wavelength of the light used, the greater is the energy of its photons. Without the optical filter, the full spectrum can be utilized wholly by the photocatalyst which will increase the photodecoloration rate. Obviously, dye removal was achieved mainly by adsorption under dark condition.

4.5. Effect of supporting electrolyte

Supporting electrolyte can interfere with photocatalytic reactions. The presence of foreign anions in the solution may affect the reaction between the organic pollutants in question and the photocatalysts. Electrolytes, especially those of hydroxyl radical scavengers, can play an important role on the degradation of organic compounds in aqueous solutions. Chloride, sulfate, and bicarbonate ions are the most common anions in natural water. The effect of NaCl, Na_2SO_4, and Na_2CO_3 on the photocatalytic decoloration of MB by Co-$BiVO_4$ was studied. Fig. 10 shows the results of MB decolorization in the presence of above electrolytes at a concentration of 0.05 mol L^{-1}. The degree of MB degradation followed the decreasing order: NaCl > Na_2SO_4 > Na_2CO_3. Although chloride appeared to exhibit a greater percentage of MB degradation than sulfate, the difference was insignificant. The decrease in the photodegradation of MB in the presence of sulfate ions might be attributed to competitive adsorption between SO_4^{2-} and MB on the surface of the photocatalyst [44]. At pH 7, both carbonate and bicarbonate ions are present. The presence of carbonate/bicarbonate ions resulted in the lowest percentage of MB removal. It has been reported that that bicarbonate and carbonate ions are a radical scav-

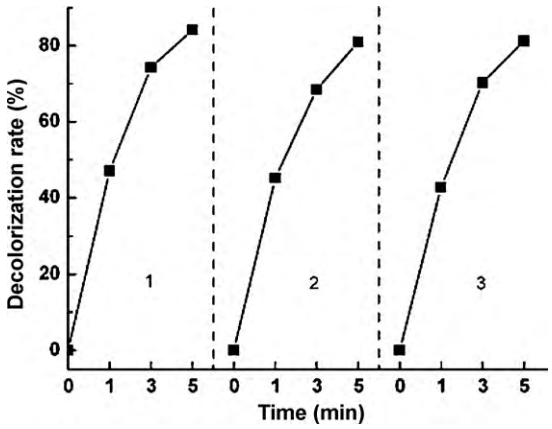

Fig. 11. Decolorization of MB by $BiVO_4$-Co(5%) photocatalyst at pH 7 in three successive cycles.

engers [45] that can trap hydroxyl radicals generated at the surface of the Co-$BiVO_4$. As the concentration of reactive radicals decreased the percentage of photocatalytic decoloration was decreased.

4.6. MB removal by reclaimed Co-$BiVO_4$ photocatalyst

To study the durability and the photostability of the nanocatalysts, Co-$BiVO_4$ powders after photocatalytic reactions were collected, dried, and reused in three successive photoreaction experiments. Fig. 11 shows results of three successive MB degradation runs using the reclaimed Co-$BiVO_4$ while keeping the experimental conditions of pH, initial MB concentration and ionic strength unchanged. It can be seen clearly from Fig. 13 that there was no loss of photocatalytic ability in three successive runs each of which lasted for 6 h. BM removal remained high at >90% in each of the three successive runs. Results demonstrated clearly that Co-$BiVO_4$ was stable and resistant to photocorrosion in the photocatalytic oxidation of organic compounds exemplified by methylene blue. Co-$BiVO_4$ photocatalysts can be applied to water purification powered by visible light.

5. Conclusion

A series of Co-$BiVO_4$ photocatalyst composites with different cobalt content were synthesized by an amorphous heteronuclear complex using diethylenetriamine pentaacetic acid (DTPA) as the chelating agent. XRD results revealed that the crystals were of the monoclinic scheelite type. Doping cobalt did not change the crystal structure of the photocatalysts. XPS results confirmed the presence of cobalt oxides in Co-BiO_4 catalysts. The valence of cobalt oxides changed from +2 to +3 when the cobalt content was increased in the composites. FESEM images revealed that the cobalt oxides were dispersed over the surface of larger $BiVO_4$ particles and became agglomerated when the cobalt content was increased. The band gap was narrowed by doping cobalt as estimated by UV–vis diffuse reflectance spectroscopy. All photocatalysts prepared exhibited photocatalytic activity upon the irradiation by visible light at $\lambda > 420$ nm. A cobalt content of 5% was the optimum condition for the preparation of the best performing Co-$BiVO_4$ photocatalysts characterized by the decolorization of methylene blue. High pH conditions favored MB decolorization. The percentage of MB decolorization increased with initial MB concentration till an optimum initial concentration of ca. 15 mg L^{-1}. Further increase in MB concentration only increased the percentage of dye decolorization slightly. The presence of simple electrolytes affects the decolorization at various extends. Chloride and sulfate had the least impact on dye decolorization. Carbonate/bicarbonate had the most adverse effect on the degradation of MB presumably by scavenging the reactive hydroxyl radicals. Results of three successive MB degradation runs using reclaimed Co-$BiVO_4$ particles indicated that the photocatalytic composites were stability toward photocorrosion with a >90% MB removal in each run.

Acknowledgements

This work was support by grants from the US Federal Administration Transit Grant (No. DE-55-7001-00), the National Natural Science Foundation of China (No. 50778172), and the Funds for Creative Research Groups of China (No. 50621804). We wish to thank our unanimous reviewers for their excellent comments and suggestions.

References

[1] J.H. Carey, Bull. Environ. Contam. Toxicol. 16 (1976) 663–668.
[2] M.R. Hoffmann, S.T. Martin, W.Y. Choi, D.W. Bahnemann, Chem. Rev. 95 (1995) 69–96.
[3] M.A. Fox, M.T. Dulay, Chem. Rev. 93 (1993) 341–357.
[4] A.L. Linsebigler, G.Q. Lu, J.T. Yates, Chem. Rev. 95 (1995) 735–758.
[5] A. Fujishima, T.N. Rao, D.A. Tryk, J. Photochem. Photobiol. C 1 (2000) 1–21.
[6] R. Asshi, T. Morikawa, T. Ohwaki, K. Aoki, Y. Taga, Science 293 (2001) 269–271.
[7] W. Choi, A. Termin, M.R. Hoffmann, J. Phys. Chem. 98 (1994) 13669–13679.
[8] H.J. Zhang, G.H. Chen, D.W. Bahnemann, J. Mater. Chem. 19 (2009) 5089–5121.
[9] A.W. Sleight, H.Y. Chen, A. Ferretti, D.E. Cox, Mater. Res. Bull. 14 (1979) 1571–1581.
[10] W.F. Yao, H. Wang, X.H. Xu, X.F. Cheng, J. Huang, S.X. Shang, X.N. Yang, M. Wang, Appl. Catal. A: Gen. 243 (2003) 185–190.
[11] H.J. Zhou, T.J. Park, S.S. Wong, J. Mater. Res. 21 (2006) 2941–2947.
[12] C.H. He, M.Y. Gu, Scripta Mater. 54 (2006) 1221–1225.
[13] C.X. Xu, X. Wei, Z.H. Ren, Y. Wang, G. Xu, G. Shen, G.R. Han, Mater. Lett. 63 (2009) 2194–2197.
[14] F. Amano, K. Nogami, B. Ohtani, J. Phys. Chem. C 113 (2009) 1536–1542.
[15] X. Zhao, J.H. Qu, H.J. Liu, C. Hu, Environ. Sci. Technol. 41 (2007) 6802–6807.
[16] J.Q. Yu, A. Kudo, Chem. Lett. 34 (2005) 1528–1529.
[17] H.M. Smith, High Performance Pigments, Wiley-VCH Verlag GmbH, Weinheim, 2002.
[18] S. Tokunaga, H. Kato, A. Kudo, Chem. Mater. 13 (2001) 4624–4628.
[19] A. Kudo, K. Omori, H. Kato, J. Am. Chem. Soc. 121 (1999) 11459–11467.
[20] D.N. Ke, T.Y. Peng, L. Ma, K. Dai, Inorg. Chem. 48 (2009) 4685–4691.
[21] W.Z. Yin, W.Z. Wang, M. Shang, L. Zhou, S.M. Sun, L. Wang, Eur. J. Inorg. Chem. (2009) 4379–4384.
[22] S.S. Dunkle, R.J. Helmich, K.S. Suslick, J. Phys. Chem. C 113 (2009) 11980–11983.
[23] L. Ge, J. Mol. Catal. A: Chem. 282 (2008) 62–66.
[24] L. Ge, Mater. Chem. Phys. 107 (2008) 465–470.
[25] S. Kohtani, J. Hiro, N. Yamamota, A. Kudo, K. Tokumura, R. Nakagaki, Catal. Commun. 6 (2005) 185–189.
[26] M. Long, W. Cai, J. Cai, B. Zhou, X. Chai, Y. Wu, J. Phys. Chem. B 110 (2006) 20211–20216.
[27] H. Xu, H.M. Li, C.D. Wu, J.Y. Chu, Y.S. Yan, H.M. Shu, Mater. Sci. Eng. B: Solid. 147 (2008) 52–56.
[28] A. Kudo, K. Ueda, H. Kato, I. Mikami, Catal. Lett. 53 (1998) 229.
[29] A.K. Bhattacharya, K.K. Mallick, A. Hartridage, Mater. Lett. (1997) 307–313.
[30] M. Long, W.M. Cai, H. Kisch, J. Phys. Chem. C 112 (2008) 548–554.
[31] K. Sayama, A. Nomura, Z.G. Zou, R. Abe, Y. Abe, H. Arakawa, Chem. Commun. (2003) 2908.
[32] H.Q. Jiang, H. Endo, H. Natori, M. Nagai, K. Kobayashi, J. Eur. Ceram. Soc. 28 (2008) 2955–2962.
[33] C.D. Wagner, W.M. Riggs, L.E. Davis, G.E. Muilenberg, Handbook of X-ray Photoelectron Spectroscopy, PerkinElmer Corporation, Minnesota, 1979.
[34] M. Lenglet, C.K. Jorgensen, Chem. Phys. Lett. 229 (1994) 616–620.
[35] H. Lin, C.P. Huang, W. Li, C. Ni, S. Ismat Shah, Y.H. Tseng, Appl. Catal. B: Environ. 68 (2006) 1–11.
[36] G.S. Li, D.Q. Zhang, J.C. Yu, Chem. Mater. 20 (2008) 3983–3992.
[37] A.P. Zhang, J.Z. Zhang, N.Y. Cui, X.Y. Tie, Y.W. An, L.J. Li, J. Mol. Catal. A: Chem. 304 (2009) 28–32.
[38] H.M. Zhang, J.B. Liu, H. Wang, W.X. Zhang, H. Yan, J. Nanopart. Res. 10 (2008) 767–774.
[39] A. Al-Futaisi, A. Jamrah, R. Al-Hanai, Desalination 214 (2007) 327–342.
[40] L.G. Devi, B.N. Murthy, S.G. Kumar, Chemosphere 76 (2009) 1163–1166.
[41] M. Schiavello, V. Augugliaro, V. Loddo, M.J. Lopez-Munoz, L. Palmisano, Res. Chem. Intermed. 25 (2) (1999) 213–227.
[42] C.J.G. Cornu, A.J. Colussi, M. Hoffmann, J. Phys. Chem. 105 (2001) 1351–1354.
[43] D.F. Ollis, E. Pelizzetti, N. Serpone, Heterogeneous Photocatalysis in the Environment: Application to Water Purification, Wiley/Interscience, New York, 1989.
[44] C. Guillard, E. Puzenat, H. Lachheb, A. Housa, J.M. Herrmann, Int. J. Photoenergy 7 (2005) 1–9.
[45] H. Xiao, R.P. Liu, X. Zhao, J.H. Qu, J. Mol. Catal. A: Chem. 286 (2008) 149–155.